Habitat International 165 (2025) 103543

Contents lists available at ScienceDirect

Habitat International

journal homepage: www.elsevier.com/locate/habitatint

Coping with the "new normal": assessing urban vibrancy resilience disparities through socioeconomic deprivation in New York City

Yunzhe Liu [a,c], Meixu Chen [b,d,*]

[a] Population Research Institute, School of Social Development, East China Normal University, China
[b] School of Social and Public Administration, East China University of Science and Technology, China
[c] MRC Centre for Environment and Health, School of Public Health, Imperial College London, UK
[d] Department of Geography and Planning, University of Liverpool, Liverpool, UK

1. Introduction

The unequal access to resources and opportunities among different geographic areas and social groups (known as socio-spatial inequality) stands as a significant barrier to sustainable urban development (Dikeç, 2001). Multiple studies from various disciplines demonstrate these disparities through their analysis of income, housing, employment, healthcare access, and environmental exposures (Chen et al., 2022; Green et al., 2021; Liu et al., 2024; Nijman & Wei, 2020; Robinson et al., 2019). Furthermore, such disparities directly influence communities' capacity to withstand and recover from disruptions, namely, the key concept of urban resilience (Amirzadeh et al., 2022; Meerow et al., 2016; Ribeiro & Pena Jardim Gonçalves, 2019; Sharifi & Yamagata, 2018).

The United Nations' SDG11 acknowledges these issues and states that urban resilience improvement is essential to developing cities that are inclusive, safe and sustainable (Acuti et al., 2020; Bautista-Puig et al., 2022; Nunes et al., 2019). Early research on urban resilience mainly focused on reinforcing physical infrastructure and economic stability, while growing evidence now reveals the critical role of human mobility and social engagement in fostering resilience (Haraguchi et al., 2022; Meerow & Newell, 2019; Yan et al., 2025). However, the impact of socioeconomic deprivation on urban vibrancy resilience (UVR) remains underexamined, despite its central relevance to advancing equitable and sustainable urban development.

Built on this context, this study seeks to create an analytical framework that can be replicated and transferred to evaluate neighbourhood resilience by exploring multidimensional socioeconomic factors that focus on social deprivation. Four objectives are proposed to accomplish our aim. First, our analysis of UVR involves examining longitudinal mobility data from pre-, peri-, and post-pandemic periods to understand both immediate disruptions and long-term recovery patterns. Second, we develop a socioeconomic deprivation index which assesses local variations throughout New York City (NYC). Third, a composite UVR index is created to measure resilience patterns throughout NYC's taxi zones. Finally, our analysis utilises a spatial econometric model to examine how socioeconomic deprivation affects UVR while considering spatial heterogeneity. The research bridges a key gap in resilience studies by merging socio-spatial inequality with UVR to provide deeper insights into urban resilience disparities.

2. Literature review

2.1. Evolving perspectives on urban resilience

The understanding of urban resilience has increasingly been shaped by two complementary perspectives: robustness and adaptivity (Schweitzer et al., 2022). Robustness focuses on structural stability which means urban systems maintain their functions even after experiencing disruptive events. Adaptivity demonstrates how urban areas employ dynamic processes to modify and restructure themselves following disturbances. Early studies concentrated on robustness to create conceptual and strategic frameworks that emphasised durable infrastructure development, long-term urban planning, and economic stability (Acuti et al., 2020; Afrin et al., 2021; Meerow et al., 2016; Newman et al., 2017; Ribeiro & Pena Jardim Gonçalves, 2019).

Urban resilience studies are now more focused on data-driven methods because new data sources, like mobility and social media information, demonstrate how communities use people's movements and social networks to adapt to city changes (Chen et al., 2024; Haraguchi et al., 2022). Chang et al. (2021) used mobile phone data to measure adaptive capability across US urban regions during COVID-19, indicating that cities with higher mobility flexibility and dispersed activity patterns recovered faster from lockdowns. Pfefferbaum et al. (2015) showed that strong social connections helped communities survive and adapt during the 1995 Chicago heatwave. Despite increased interest in

* Corresponding author. School of Social and Public Administration, East China University of Science and Technology, Shanghai, China.
E-mail address: maychen@ecust.edu.cn (M. Chen).

https://doi.org/10.1016/j.habitatint.2025.103543
Received 7 November 2024; Received in revised form 4 August 2025; Accepted 5 August 2025
Available online 12 August 2025

these issues, the combined impact of human mobility and socioeconomic disparity on neighbourhood-level adaptation is understudied, limiting our knowledge of the dynamic mechanisms driving urban resilience during extended shocks.

2.2. Conceptualisation of urban vibrancy resilience

Urban vibrancy refers to the dynamic liveliness of urban spaces, driven by economic activity, social engagement, and land-use diversity (Jacobs, 1961; Yue et al., 2017). Urban vibrancy serves as a crucial indicator of urban well-being, since lively cities foster innovation, cultural interchange, and economic growth (Chen et al., 2019). Researchers have examined urban vitality by evaluating land-use variety and public space activity through human mobility patterns (Liu et al., 2021; Tu et al., 2020). However, the resilience of urban vibrancy against disruptions remains an understudied topic.

The COVID-19 pandemic revealed a drop in urban vibrancy as mobility restrictions coupled with economic difficulties and social isolation led to the need for research into UVR. The UVR expands traditional urban resilience theory through an investigation of changes in human activity and mobility patterns during unforeseen urban disruptions (Chen et al., 2024; Liu, Wang, et al., 2023). The concept becomes essential for addressing socioeconomic inequalities as marginalised groups typically experience more severe disturbances to their movement and social ties during times of crisis.

2.3. Urban vibrancy resilience studies since COVID-19

The pandemic has triggered lasting urban adaptations including remote work, hybrid commuting, online education, and digital commerce, which continue to influence the post-pandemic "new normal" era (Florida et al., 2021; Huang & Li, 2022). Recent studies have examined how urban areas resist the COVID-19 pandemic alongside the impacts of socioeconomic elements on their resilience (Florida et al., 2021). researched urban recovery from the COVID-19 pandemic through analysis of mobility and economic activity variations over time. Ntounis et al. (2022) conducted a quantitative analysis to understand how income differences affected city vibrancy. The research by Valenzuela--Levi et al. (2021) demonstrated how employment changes create uneven spatial effects on urban vibrancy. Xiao and Liu (2023) and Zhang and Wang (2023) investigated human mobility alongside public engagement and spatial variability and found that area vibrancy varies significantly based on the socioeconomic conditions.

However, most current research examines socioeconomic factors separately without addressing their interconnected effects on UVR. Designing equitable resilience strategies requires thorough analysis of the relationship between multidimensional socioeconomic factors and the adaptivity of urban vibrancy.

2.4. Research gaps

Current studies have improved urban resilience knowledge, but significant research gaps still exist. First, most studies failed to conduct comprehensive long-term evaluations to monitor the entire development of vibrancy resilience. They tended to capture short-term data points, or "snapshots", rather than tracking continuous changes from pre-pandemic to post-pandemic periods, which limits our understanding of extended adaptation and recovery patterns (Florida et al., 2021). Second, current research examines city and regional scales but overlooks detailed neighbourhood-level investigations (Ntounis et al., 2022; Valenzuela-Levi et al., 2021). Small-area assessments are needed for targeted interventions because resilience dynamics function at highly localised levels, which exhibit spatial differences. Most importantly, the current research fails to examine how socioeconomic elements interact with each other while assessing their influence on UVR (Alizadeh & Sharifi, 2021; Pfefferbaum et al., 2015). The multidimensional nature of resilience demands that urban planning employs a comprehensive analytical framework which combines socioeconomic deprivation factors with human mobility and spatial dynamics. To effectively address these gaps, we need a replicable data-driven framework which captures UVR's spatiotemporal dimensions while examining socioeconomic inequalities' effects on resilience at detailed spatial levels.

3. Data

3.1. Study area and period

New York City (NYC), comprising the boroughs of Brooklyn, Queens, Manhattan, the Bronx, and Staten Island, emerged as the world's first megacity in the 1930s and remains the most populous urban centre in North America (Gross & Savitch, 2023). The reasons for its selection as our case study are threefold. First, its exceptional population density, intricate urban built environment, and diverse sociodemographic composition collectively make it an ideal "natural laboratory" for examining heterogeneous urban dynamics. Second, NYC was an early epicentre of the COVID-19 pandemic in the US (Thompson et al., 2020), subject to three government-mandated lockdowns (in March 2020, November 2020, and January 2021) that severely disrupted daily life and urban functionality, revealing the vulnerabilities of typical metropolitan areas. Lastly, the city's robust open-data infrastructure (e.g., NYC Open Data[1]) enables in-depth, neighbourhood-level UVR analyses. Publicly accessible datasets - spanning mobility records, sociodemographic information, and land-use data-provide a solid foundation for integrating mobility metrics with contextual variables, thus offering deeper insights into the ways diverse neighbourhoods adapt and recover following urban shocks.

The research timeline spans 52 months, starting from September 1, 2019 and ending on December 31, 2023, to cover all phases of the COVID-19 timeline, including the pre-pandemic, peri-pandemic and the "new normal" period. By using this longitudinal approach, investigations can be performed through both recovery processes and pandemic effects while also gaining an in-depth understanding of UVR dynamics throughout these essential times.

3.2. Mobility data and taxi zones

For-Hire Vehicle (FHV) trip data were used to represent urban vibrancy in this study. FHV data, comprising NYC's traditional FHV vehicles, Uber, Lyft, Juno, and Via services, has transformed NYC's transportation system, surpassing 100,000 vehicles in 2019 and displacing traditional yellow and green taxis (Roberton et al., 2020). By 2019, FHVs accounted for approximately 76 % of all TLC-regulated trips, making them a city-wide and ubiquitous service with a uniform data structure across all five boroughs. The substantial increase in daily FHV trips from 439,000 in 2017 to 701,000 in 2019, alongside its consistent longitudinal signal, established this dataset as a valuable foundation for investigating dynamic urban activity (Blasio & Jarmoszuk, 2020).

The FHV industry in NYC was hit severely due to the disruption from the COVID-19 pandemic (NYC TLC, 2020). The city announced a state of emergency just days after logging its first COVID-19 case on March 1, 2020 while ordering extensive shutdowns of non-essential businesses and travel. Consequently, the FHV sector has experienced a marked decline in activity since it heavily depends on business, tourism and daily commuting. Subsequently, as restrictions were gradually eased and the city slowly adapted to the new conditions, many FHV drivers diversified their services by taking on food delivery roles under the city's GetFood programme (Pereira, 2020). By June 2020 FHV trips climbed roughly 78 % since their lowest point but still stayed 71 % beneath the

[1] https://opendata.cityofnewyork.us/.

levels they reached in June 2019 before the pandemic struck (NYC TLC, 2020). The significant downturn followed by gradual recovery in FHV activity shows how urban systems adapt and provides useful context for studying UVR throughout the COVID-19 pandemic.

FHV trip data were collected from the NYC Taxi and Limousine Commission (TLC) data repository[2], which were constructed using the NYC Department of City Planning's Neighbourhood Tabulation locations data to accurately display locations and better assess passenger pick-up and drop-off (NYC TLC, 2019). TLC has divided the city into 263 distinct taxi zones (262 zones are located within the five boroughs of NYC), each assigned a specific number. The data is recorded daily and contains rows that reflect unique FHV trips. Each trip is identifiable by TLC taxi zone IDs for the pick-up and drop-off locations and includes timestamps. Starting in the second half of 2016, these locations were designated using taxi zone IDs instead of GPS coordinates due to privacy considerations.

A "temporal profile" for each taxi zone was created by aggregating daily FHV pick-ups and drop-offs, capturing the dynamic nature of urban vibrancy over the five-year study period. To smooth out daily fluctuations and remove seasonality impacts, a seasonal-trend decomposition procedure based on Loess (STL) was applied, producing a smoothed curve that reflects the general half-year (180-day) urban vibrancy trend in NYC (Rojo et al., 2017). Fig. 1 illustrates the spatial distribution of TLC taxi zones and their smoothed trend curves across NYC's five boroughs.

3.3. American community survey data

The research utilises the most recent five-year American Community Survey (ACS) estimates from 2022 at the Census Tract level released by the US Census Bureau to depict NYC's socioeconomic conditions. The ACS serves as a rolling survey which took the place of the long-form decennial census in 2010 to deliver yearly information on US demographic, social, economic, and housing patterns. While this continuous collection process ensures relatively up-to-date information, its complex sampling design and small sample size can lead to estimation inaccuracies, particularly in smaller geographic areas (Spielman & Singleton, 2015).

We utilise these ACS data to derive key socioeconomic indicators reflecting aspects of living conditions, vehicle availability, employment and related factors for constructing the Carstairs Index (CI). Such variable selection is guided by the established CI framework, which will be elaborated in more depth in the methodology section. Furthermore, additional demographic variables are extracted from the ACS data and incorporated as covariates in the subsequent analysis.

4. Methods

Our study introduces a dual-layer analytical structure which examines UVR through the lens of multidimensional socioeconomic deprivation, thereby addressing key gaps in existing research. Fig. 2 displays the essential framework structure. The first layer, termed the socioeconomic deprivation layer, utilises the well-established CI to measure material disadvantage across NYC's taxi zones. The second layer, known as the urban vibrancy layer, constructs a composite UVR Index (UVRI) by analysing FHV mobility data. Both indices are then integrated within a Geographically Weighted Regression (GWR) model, where UVRI serves as the dependent variable and CI is the principal explanatory variable, alongside demographic, land-use and accessibility covariates derived from multiple NYC open-data sources. Since all datasets utilised in this study are openly available, the proposed framework is both reproducible and transferable to other urban contexts, thus offering significant contributions to the existing literature on urban resilience. The following subsections provide an in-depth discussion of each layer.

4.1. Socioeconomic deprivation layer

This research uses the CI, originally developed by (Carstairs & Morris, 1990), as a composite measure to systematically examine the socioeconomic deprivation across NYC at the TLC taxi zone level. The CI includes four census domains, namely, overcrowding, male unemployment, lack of car ownership and low social class. This well-established method has been extensively applied in spatial epidemiology and public health research across different geographic scales (Anna et al., 2013; Buckingham et al., 2021; Fecht et al., 2018).

All four CI domains were obtained from the 2022 ACS five-year estimates at the Census Tract level (see Table 1 for variable definitions). Because ACS data are not published at the TLC taxi-zone scale, we aggregated tract-level values to taxi zones using an area-weighted averaging approach. To avoid bias from areas with minimal residential populations, zones dominated by major airports (i.e., Newark, LaGuardia, JFK), large parks (e.g., Central Park, Pelham Bay Park, Bronx Park), and other uninhabited areas (e.g., Rikers Island, Randall's/Wards Island) were excluded. Following this filtering, 234 of the 263 TLC taxi zones remained for CI calculation.

For a certain TLC taxi zone i, the CI can be calculated by the following formula (Carstairs & Morris, 1990):

$$CI_i = \sum_{c=1}^{n} Z_i^c$$

Where n denotes the number of selected ACS variables, which totals four. Z_i^c is the z-score value for each census variable c, calculated as follows (Kreyszig, 2011):

$$Z_i^c = \frac{X_i^c - \mu_c}{\sigma_c}$$

Where X_i^c is the value of census variable c in the area of interest i. μ_c is the mean value across all TLC Taxi Zones for that variable, and σ_c is the standard deviation.

4.2. Urban vibrancy layer

We adapt the framework originally developed by Nan & Sansavini (2017) to systematically quantify UVR. In the adapted conceptual diagram (Fig. 3), the x-axis represents time, covering the study period from 2019 to 2023, which is divided into three phases: pre-pandemic, peri-pandemic (subdivided into Impact and Recovery stages), and post-pandemic (i.e., the new normal). The y-axis represents the standardised urban vibrancy level for each TLC taxi zone, presented as an index. A baseline value of 100 corresponds to the average vibrancy level measured over a 180-day period prior to the COVID-19 pandemic (see the red dashed line in Fig. 3). This relative index enables each value to be interpreted as a percentage of pre-pandemic conditions; for example, a score of 50 implies 50 % of the baseline vibrancy, while a score of 200 indicates that vibrancy has doubled. The observed U-shaped curve reflects the initial reduction in urban vibrancy due to the COVID-19 pandemic and its associated mobility restrictions, followed by fluctuations during the Recovery stage caused by subsequent pandemic waves and policy interventions. Although the post-pandemic average (indicated by the blue dashed line) is not necessarily lower than the pre-pandemic level in theory, in most cases it remains lower, while some zones even surpass the pre-pandemic baseline.

A composite index was constructed from four metrics derived from the smoothed resilience curve to assess UVR quantitatively. Each metric is designed to capture different aspects of the resilience process.

[2] https://www.nyc.gov/site/tlc/about/tlc-trip-record-data.page.

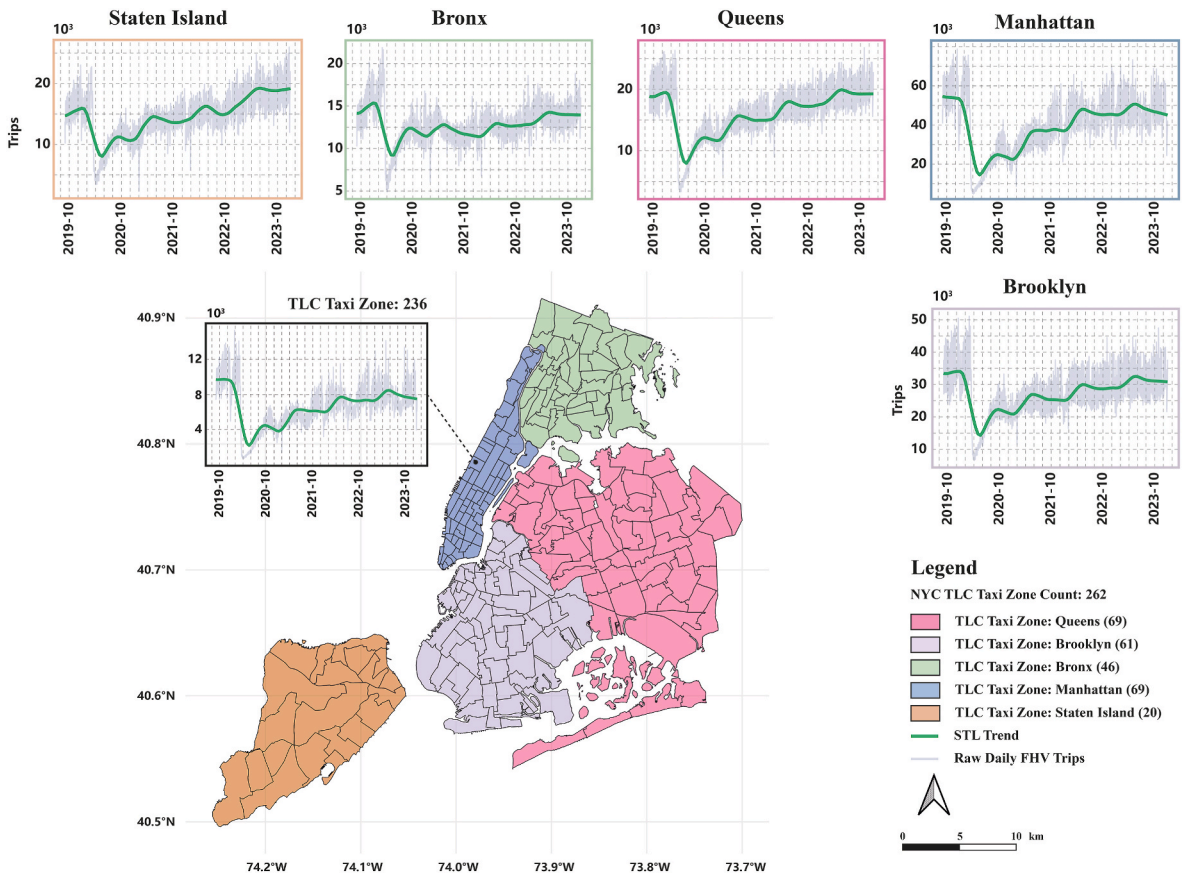

Fig. 1. Daily raw and STL-smoothed FHV trip counts in each of NYC's five boroughs (2019–2023), accompanied by a borough-level map showing the TLC taxi zones.

1) **Impact Range (IR):** This metric computes the most significant reduction in urban vibrancy since the pandemic outbreak by calculating the maximum deviation between the lowest point of urban vibrancy and the pre-pandemic baseline.

$$IR_i = UV_i^{T1} - UV_i^{T0}$$

Where IR_i represents the Impact Range in taxi zone*i*. UV_i^{T0} denotes the urban vibrancy in that taxi zone over a 180-day period prior to the outbreak day ($T0$), serving as the baseline. UV_i^{T1} is the urban vibrancy at its lowest point during the pandemic, identified independently, and $T1$ represents the time at which this minimum occurs.

2) **Impact Pace (IP):** This metric measures the rate of decline in urban vibrancy from the pre-pandemic baseline to its lowest point, computed as the slope of the declining curve.

$$IP_i = \frac{UV_i^{T1} - UV_i^{T0}}{T_1 - T_0}$$

Where IP_i represents the Impact Pace in taxi zone *i*. The results illustrate the immediate and severe impacts of the pandemic, which was presented as a daily percentage.

3) **Recovery Pace (RP):** This metric quantifies how quickly urban vibrancy rebounds from its lowest point to a recovery phase.

$$RP_i = \frac{UV_i^{T2} - UV_i^{T1}}{T_2 - T_1}$$

Where RP_i represents the Recovery Pace in taxi zone *i*. UV_i^{T2} is the vibrancy at a later point indicative of recovery, and $T2$ is the time associated with this urban vibrancy. The result quantifies how quickly and effectively urban areas adapt to post-pandemic conditions, averaged by each day.

4) **Rebound Ratio (RR):** This metric measures the recovery of urban vibrancy by comparing current levels to those before the pandemic.

$$RR_i = \frac{UV_i^{T2}}{UV_i^{T0}} * 100$$

Where RR_i represents the Rebound for taxi zone *i*. The resulting percentage indicates the extent of recovery, with values above 100 showing that vibrancy has surpassed pre-pandemic levels, values exactly 100 indicating a return to prior conditions, and values below 100 denoting that recovery is not yet complete.

As illustrated in Fig. 3, three key time points (i.e., T_0, T_1, and T_2) are required to derive the four metrics of resilience. T_0 corresponds to March 1, 2020, when NYC confirmed its first COVID-19 case, marking the onset of pandemic disruption. T_1 is defined as the lowest point in the smoothed vibrancy trends of each taxi zone, which represents the greatest disruption to mobility. On February 10, 2023, NYC ended its vaccine mandate for city workers and began easing other pandemic restrictions, initiating the "new normal" phase. However, because urban vibrancy did not immediately stabilise, we used a plateau detection algorithm (Wang & Wang, 2006) to determine T_2 for each taxi zone. Specifically, the algorithm identifies the first plateau occurring on or after February 10, 2023 that meets two criteria: The plateau detection algorithm required a daily variance tolerance of 0.05 along with a sequence of at least 15 consecutive days. The calculated T_2 dates for each zone represent the point at which local vibrancy reached a stable post-pandemic equilibrium.

Following identification of T_0, T_1, and T_2, we computed four resilience metrics (i.e., *IR*, *IP*, *RP*, and *RR*) from each taxi zone's smoothed

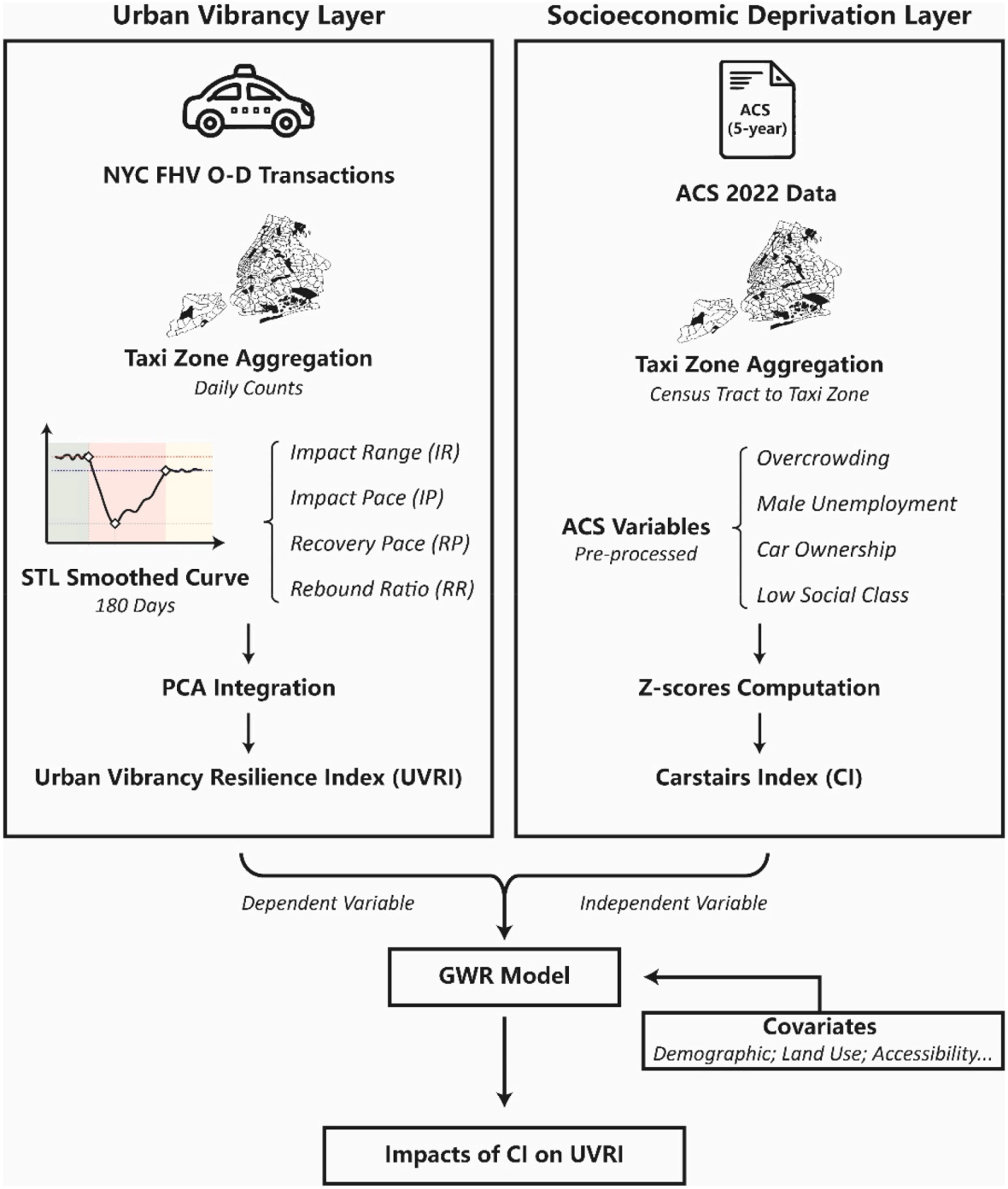

Fig. 2. Two-layer analytical framework for assessing UVR, integrating FHV-based UVRI and ACS-based CI with a GWR model.

vibrancy trend. To compile these metrics into a composite UVRI, Principal Component Analysis (PCA) was applied. PCA reduces a set of correlated variables into orthogonal principal components, thereby decreasing dimensionality while retaining the greatest share of variance (Jolliffe, 2002). We chose PCA over alternatives such as factor analysis or multidimensional scaling because it is computationally straightforward, yields transparent variable loadings that clarify each metric's contribution, and imposes minimal modelling assumptions (Jollife & Cadima, 2016). The first principal component, which explains the largest proportion of variance, constitutes our composite Urban Vibrancy Resilience Index (UVRI). For each taxi zone i, UVRI is calculated as:

$$UVRI_i = PCA_1(IR_i, IP_i, RP_i, RR_i)$$

Where PCA_1 denotes the first principal component. IR_i, IP_i, RP_i, and RR_i are the values of four metrics computed at each taxi zone *i*.

4.3. Relationships between socioeconomic deprivation and UVR

We first examined the global association between the socioeconomic deprivation (measured by CI) and the UVR (measured by UVRI) across 234 TLC taxi zones, using Pearson correlation and a correlation matrix of CI, UVRI, and their constituent metrics. However, a global measure such

Table 1
Socioeconomic variables selected from the 2022 ACS for the construction of CI.

Domains	Measure	Variable	Description
Overcrowding	Occupants Per Room	>1 occupant per room	% of households with more than 1 occupant per room
Unemployment	Employment Status	Unemployed male	% of male population in the labour force who are unemployed
Lack of car ownership	Vehicles Available	No vehicle	% of households with no vehicle available
Low social class	Poverty Status	Below poverty level	% of population with income in the past 12 months below the poverty level

as Pearson's correlation assumes uniformity across space and therefore cannot capture geographic variation.

To investigate spatial clustering of UVRI, we calculated Moran's I and Local Indicators of Spatial Association (LISA). Moran's I provides a single statistic to determine whether similar UVRI values cluster beyond random chance (Getis, 2007; Moran, 1950), while LISA identifies local hotspots and cold spots at a finer level (Anselin, 1995). Constructing a spatial weights matrix was critical for these spatial analyses, but NYC's fragmented geography posed certain challenges. To address this, we adopted a hybrid approach. In contiguous parts of the city, we directly employed the Queen contiguity method, which defines taxi zones sharing any boundary point as neighbours. In contiguous parts of the city, we directly employed the Queen contiguity method, which defines taxi zones sharing any boundary point as neighbours. For those areas lacking direct contiguity, we applied a k-nearest neighbours (KNN) approach to form the neighbourhood matrix. The number of k was set to five based on the average number of neighbours observed in most taxi zones. This combined method ensured that each zone retained sufficient spatial connections for robust inference. Following the definition of this weights matrix, permutation-based tests ($p < 0.05$) were carried out for Moran's I and LISA, thereby establishing whether any observed clustering of UVRI values diverged significantly from random distributions.

Spatial autocorrelation analysis shows where UVRI clusters but fails to explain how the relationship between CI and UVRI changes between different neighbourhoods. We therefore adopted GWR to capture spatial non-stationarity in the link between socioeconomic deprivation and UVR (Fotheringham et al., 2002). In contrast to ordinary least squares (OLS) and other spatial econometric models (e.g., spatial lag or error models), which largely address spatial dependence without producing localised estimates, GWR provides location-specific regression coefficients by calibrating individual regressions for each observation area. This methodological advantage has been demonstrated in studies across multiple domains where spatial patterns matter, such as environmental justice and pollution exposure (Chakraborty et al., 2022), housing studies (Duan et al., 2021; Z. Huang et al., 2017), human mobility dynamics (Jin et al., 2019; Y. Wang et al., 2019), public health (Khedmati Morasae et al., 2024; Su et al., 2017), and urban resilience (Liu, Gu, et al., 2023; H. Wang et al., 2023).

The GWR specification defines UVRI as the dependent variable and CI as the primary explanatory factor. Based on established research within similar urban settings (Liu et al., 2020; Liu, Gu, et al., 2023), we include demographic factors (ethnic groups), built environment features (land use types), and accessibility measures (distance to the nearest transit stop, street intersection density, and employment-household entropy) to enhance model robustness. All these covariates of GWR were sourced from the NYC Open Data Platform, enabling a comprehensive and data-driven representation of the local factors influencing neighbourhood resilience. Based on the study of (Fotheringham et al., 2002), the GWR model can be expressed as:

$$UVRI_i = \beta_0(u_i, v_i) + \beta_1(u_i, v_i)CI_i + \beta_2\,(u_i, v_i)X_{2,i} + \ldots + \beta_k\,(u_i, v_i)X_{k,i} + e_i$$

where $UVRI_i$ signifies the UVRI at taxi zone i, CI_i indicates the CI at zone i, and $X_{2,i}$ to $X_{k,i}$ represent other covariates. The spatial coordinates (u_i, v_i) determine the local regression coefficients from β_0 to β_k, while e_i represents the error component. We used the corrected Akaike Information Criterion (AIC) (Su et al., 2012) to ascertain the bandwidth for the GWR model, thereby guaranteeing optimal model performance. The resulting local coefficient estimates illustrate the geographical heterogeneity of socioeconomic deprivation's impact on UVR across various neighbourhoods in NYC.

5. Results

5.1. Disparities of social deprivation

Fig. 4 shows the CI across NYC's TLC taxi zones and displays

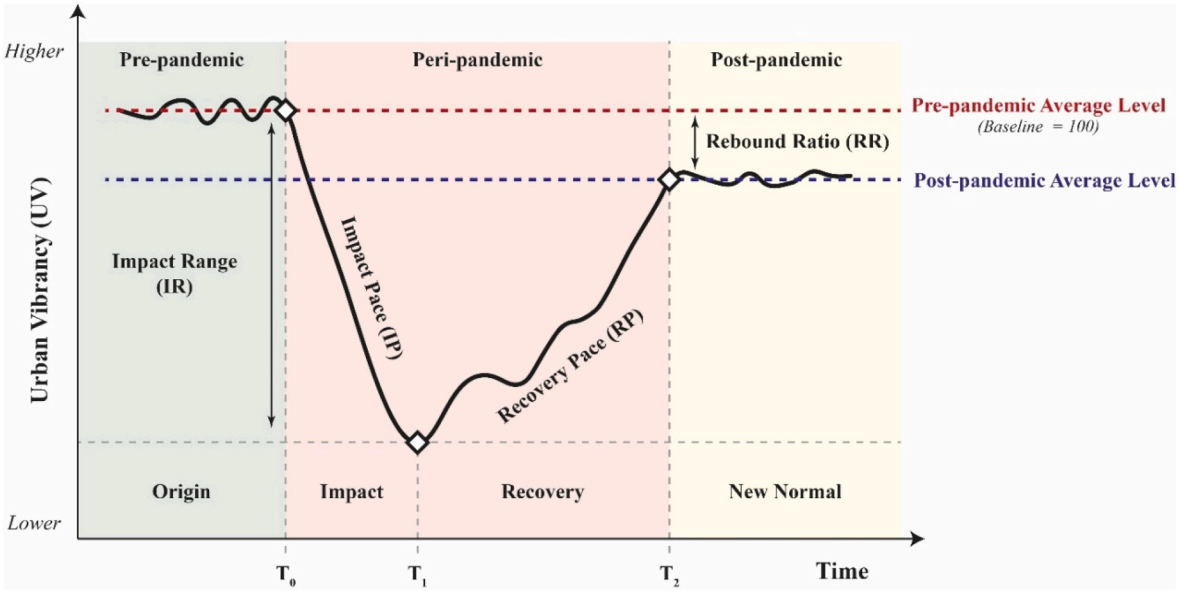

Fig. 3. Conceptual resilience curve to measure UVR in NYC.

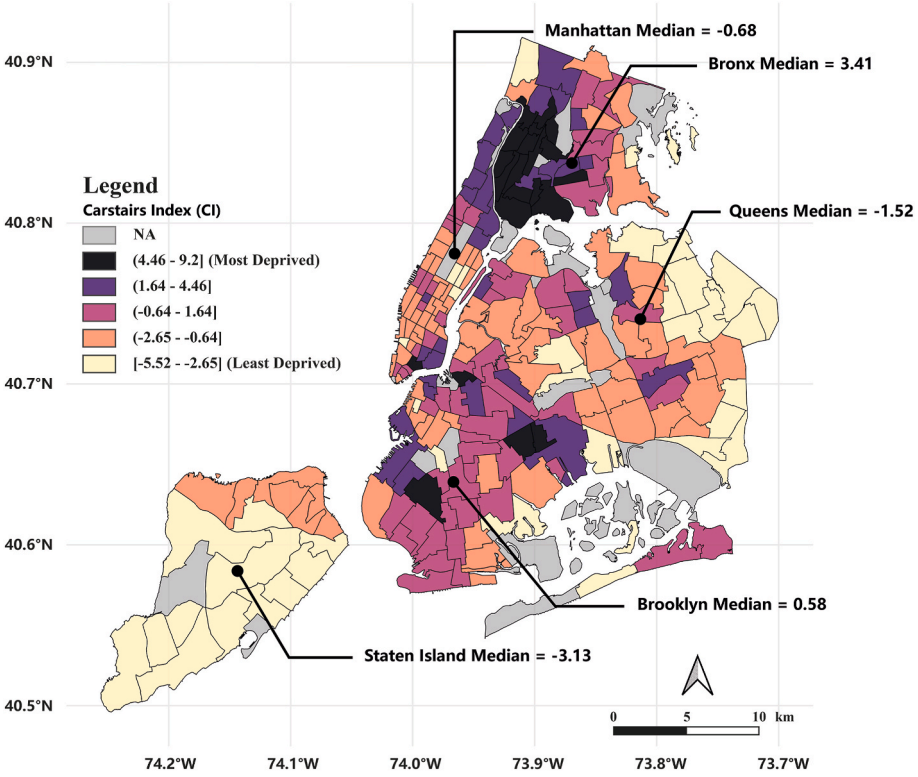

Fig. 4. Spatial distribution of the CI across NYC's TLC taxi zones, with borough-stratified median values.

significant differences in socioeconomic status. The darker colour tones represent areas with greater deprivation, while the lighter colour tones show relatively wealthier locations. The CI range between −5.52 and 9.2 indicates major differences in urban living conditions. A borough-level stratification of CI medians further illustrates these divergences. The Bronx posts the highest median at 3.41, followed by Brooklyn at 0.58, Manhattan at −0.68, Queens at −1.52, and Staten Island at −3.13.

Zones featuring notably high CI values (i.e., severe deprivation) tend to cluster in northern Manhattan and substantial sections of the Bronx, with additional concentrations evident in parts of Brooklyn. In contrast, neighbourhoods with lower CI scores, which indicate relative wealth, primarily exist on Staten Island, eastern Queens, and sections of lower Manhattan, including Midtown and the Upper East Side.

5.2. *Spatial patterns of urban vibrancy resilience*

A series of maps in Fig. 5 illustrates the spatial distribution of the four UVR metrics (IP, IR, RP, and RR) across NYC, highlighting disparities in the neighbourhood's ability to withstand and recover from pandemic-related disruptions. Fig. 5(a) and (b) are both represented by negative values, with darker colours signifying a faster decline and a greater impact, respectively. The most severe impacts and accelerated reduction in urban vibrancy are observed in middle and lower Manhattan, northeast Queens, and southern Staten Island, whereas the Bronx, eastern Brooklyn, and southern and eastern Queens show a slower fall and lesser impacts, indicating a more progressive decline.

Fig. 5(c) highlights the variability in recovery speeds across different areas of the city, where darker colours indicate a faster pace of recovery from the pandemic's impact. The overall spatial patterns align with those of IP and IR, where middle and lower Manhattan, northeast Queens and southeast Brooklyn show the most rapid recovery since the pandemic outbreak. In addition, most areas in Staten Island also illustrate faster recovery. These regions' resilience is demonstrated by their quick return to pre-pandemic levels of urban vibrancy. The slower recovery areas are found in the areas where slower reduction and smaller impacts are identified in Fig. 5(a) and (b).

The spatial patterns of Fig. 5(d) differ slightly from other metrics. Over half (i.e., 57 %) of taxi zones show higher RR values, which illustrates a holistic resilient rebound in NYC. Green areas in Staten Island, eastern Queens, and lower Manhattan indicate that the recovery of urban vibrancy has surpassed the pre-pandemic levels. Conversely, pink shades with RR values less than 97.3 suggest a "new normal" for these areas has not yet attained past urban vibrancy. These areas are primarily found in central and northern Manhattan, the southern Bronx, and Brooklyn's central and southeastern parts. Zones that have returned to pre-pandemic levels are represented by white-coloured areas, which are primarily scattered throughout the Bronx, Brooklyn, and Queens.

The spatial distribution of the computed UVRI is presented in Fig. 6 (a), where higher values (shades of yellow) denote greater resilience, while lower values (dark blue) signify lower resilience. Fig. 6(b) and (c) demonstrate how UVRI is computed by using the PCA approach. The UVRI in Fig. 6(a) spans from −3.54 to 3.4, signifying substantial spatial variability in the resilience of urban vitality throughout NYC. Manhattan displays the greatest median UVRI (1.73), with notably elevated spatial concentration in lower and central Manhattan, significantly enhancing its overall resilience. The majority of Staten Island exhibits relatively high resilience with the second-highest median UVRI (0.55), except for its northeast points. Northeast and west Queens, as well as northwest Brooklyn, contain additional small-scale zone concentrations with elevated UVRI. The Bronx has the lowest median UVRI (−2.31) of all boroughs, suggesting that it is extremely challenging to maintain urban vibrancy during COVID-19. Southeast Brooklyn, northern Manhattan, and southeast Queens are also home to low-value aggregations, which hinder the vibrancy of the urban environment in these communities.

Fig. 6(b) illustrates the eigenvalues and cumulative variance explained by the first four principal components. According to the diagram, the first principal component (PC1) solely explains a substantial 67 % of the total variance, effectively capturing most of the essential information from the original UVR metrics. PC1, which captures most variance, is used to build the UVRI, while the second principal

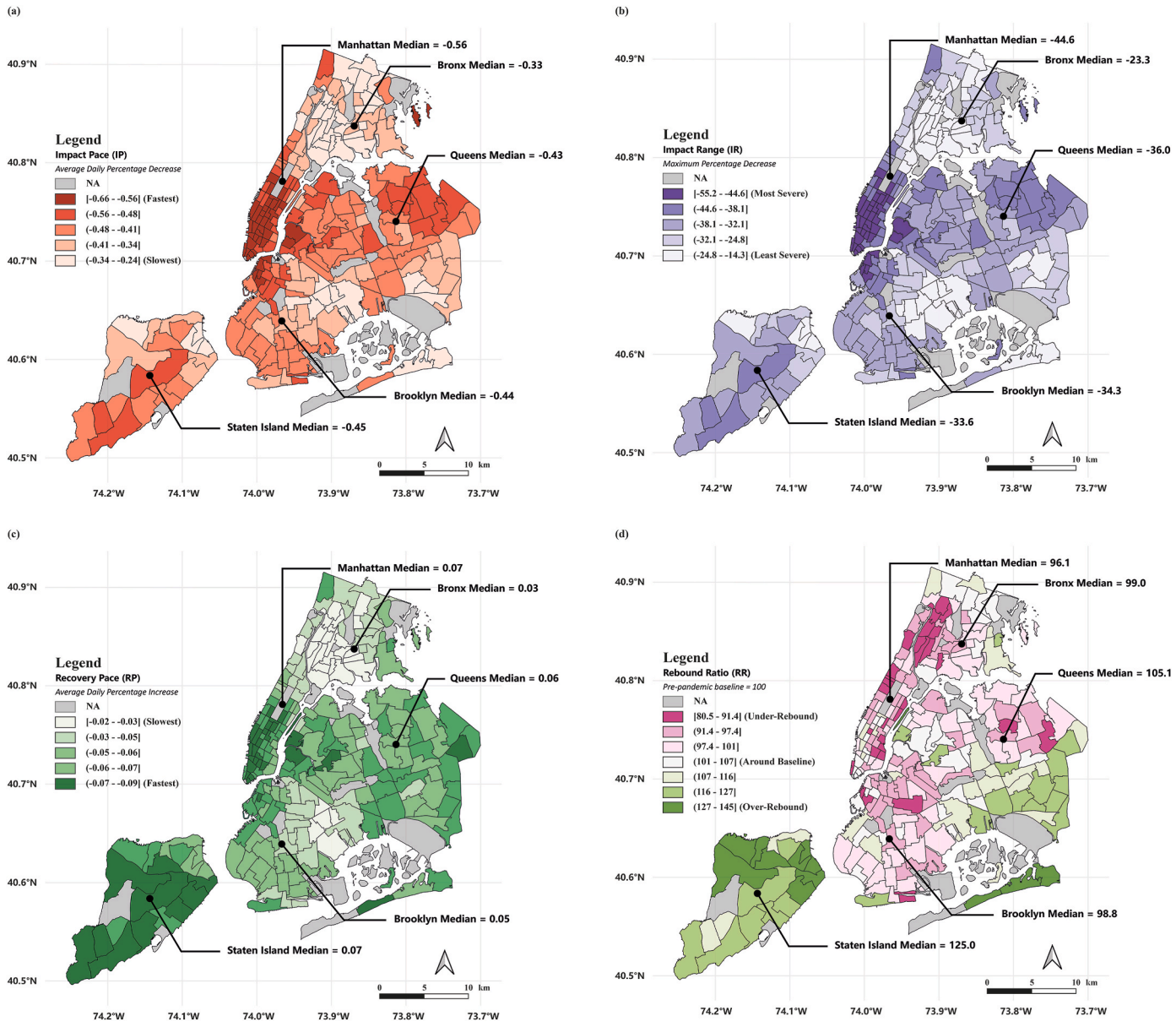

Fig. 5. Spatial distribution of the four UVR components across NYC's TLC taxi zones, with borough-stratified median values: (a) Impact Pace (IP), (b) Impact Range (IR), (c) Recovery Pace (RP), and (d) Rebound Ratio (RR).

component, which explains 31.8 % variation, captures mainly residual variance. Fig. 6(c), the PCA biplot, further highlights the relative contributions of each original metric to the first two principal components. IR and IP both display significant negative impacts on PC1, which approaches −1, whereas RP demonstrates a strong positive association with PC1 at approximately 0.9. These indicate that regions with high UVRI values show slower and less intense disturbances but demonstrate faster recovery rates. RR produces a negligible impact on PC1, while the other three metrics demonstrate more significant effects. Instead, RR shows a strong negative influence on PC2, which indicates that its pattern in UVR behaviour differs from IR, IP and RP. This biplot clearly illustrates how impact degrees alongside recovery speed influence the resilience patterns across NYC taxi zones, enhancing the interpretability and transparency of UVRI.

5.3. Global and local relationships between CI and UVRI

Fig. 7 presents a correlation matrix that showcases the global Pearson correlations among the UVRI components and the CI across NYC's TLC taxi zones. Overall, UVRI correlates significantly and negatively with CI ($r = -0.6$, $p < 0.001$). This indicates that areas with a higher level of resilience are more likely to exhibit lower socioeconomic disadvantage. Particularly, the correlations between UVRI and two of CI's constituent measures, UM and BP, show the same high negative associations ($r = -0.66$, $p < 0.001$). This result highlights the crucial role of economic stability in supporting resilience fostering. Consequently, communities characterised by higher unemployment or a greater proportion of the population living below the poverty line appear less capable of sustaining vibrancy during disruptions.

As mentioned earlier, the Pearson correlation does not consider spatial dependencies. Accordingly, we explore UVRI's spatial autocorrelation to reveal its spatial pattern. The analysis results that include the Moran's I scatter plot (b), LISA cluster map (a), and LISA significance map (c) are presented in Fig. 8. The Moran's I score of 0.804 indicates a relatively high positive spatial autocorrelation, suggesting that zones with high UVRI tend to be surrounded by other high-resilience areas, and vice versa. This reinforces the necessity of employing a GWR model to consider localised spatial variations in the subsequent relationship

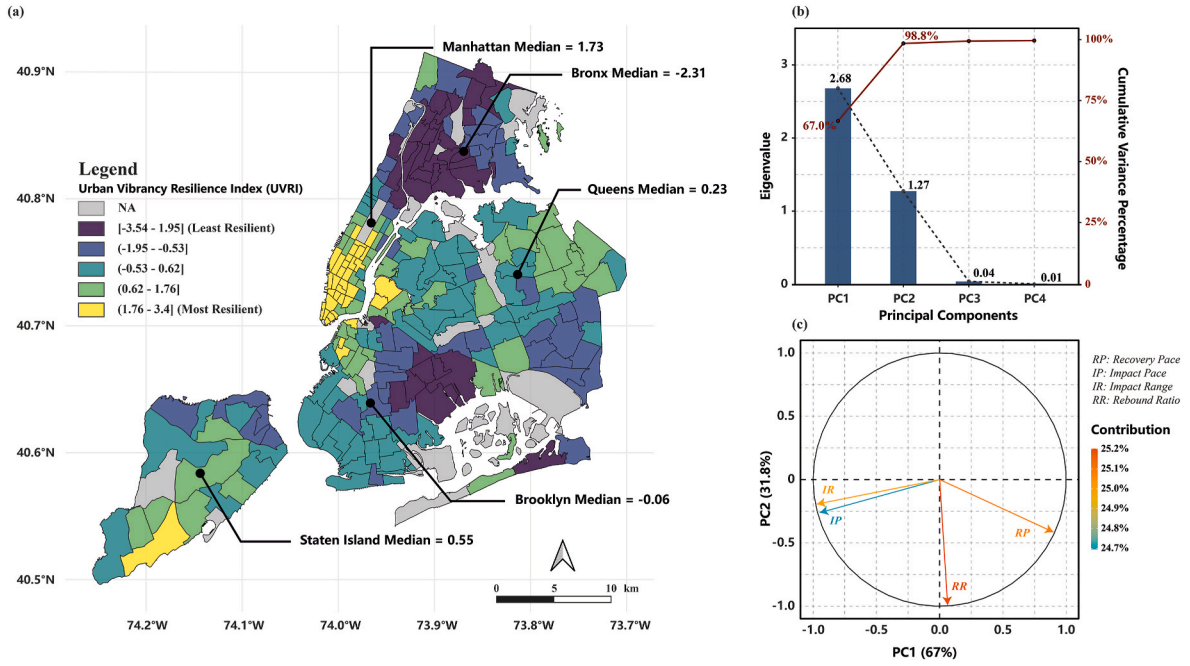

Fig. 6. (a) Spatial distribution of the UVRI across NYC's TLC taxi zones with borough-stratified median values. (b) Scree plot showing eigenvalues and cumulative variance explained by the first four principal components. (c) PCA biplot illustrating the contributions and correlations of four UVR components (IP, IR, RP, RR) with the first two principal components.

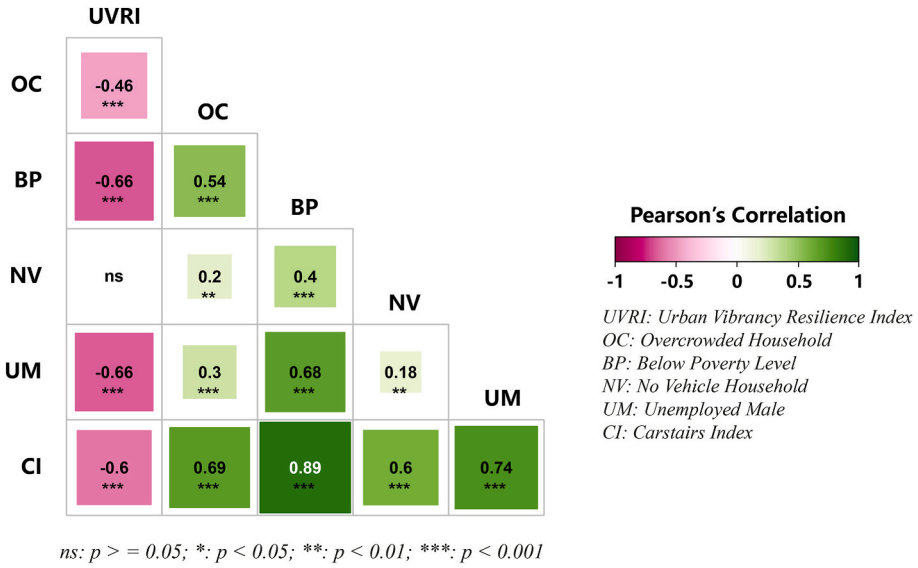

Fig. 7. Pearson correlation matrix between the UVRI and CI components. Cell colours represent correlation strength and direction; significance levels are denoted by asterisks (*p < 0.05; **p < 0.01; ***p < 0.001), with "ns" indicating non-significance. (For interpretation of the references to colour in this figure legend, the reader is referred to the Web version of this article.)

analysis.

The LISA cluster map shows the different UVRI levels in different TLC taxi zones by showing where the statistically significant high- and low-resilience clusters are grouped together. Overall, a total of 77 taxi zones demonstrates significant local spatial autocorrelation with p-values below 0.05. Within these statistically significant clusters, High–high (HH) clusters, indicating resilient hotspots, are primarily located in middle and lower Manhattan, northwest Brooklyn, southern Staten Island, and northeast Queens. Conversely, low–low (LL) clusters, representing resilience cold spots, mainly appear in the Bronx, northern Manhattan, and southeast Brooklyn.

The results from the spatial autocorrelation analysis confirmed the presence of spatial dependencies, prompting the use of an adjusted GWR model to examine how the relationship between local contextual factors and UVR varies across neighbourhoods. Fig. 9 presents the GWR results. The local coefficients for CI shown in Fig. 9(a) display negative values for every borough, which indicates that areas with higher levels of socioeconomic deprivation experience reduced UVRI. However, the strength of this relationship varies geographically. The most pronounced negative effects are found in Brooklyn (median = −0.41) and Queens (−0.37), as indicated by darker shaded areas. In contrast, Manhattan (−0.26), the Bronx (−0.28), and Staten Island (−0.31) show comparatively weaker relationships, pointing to spatial heterogeneity in how deprivation influences vibrancy resilience.

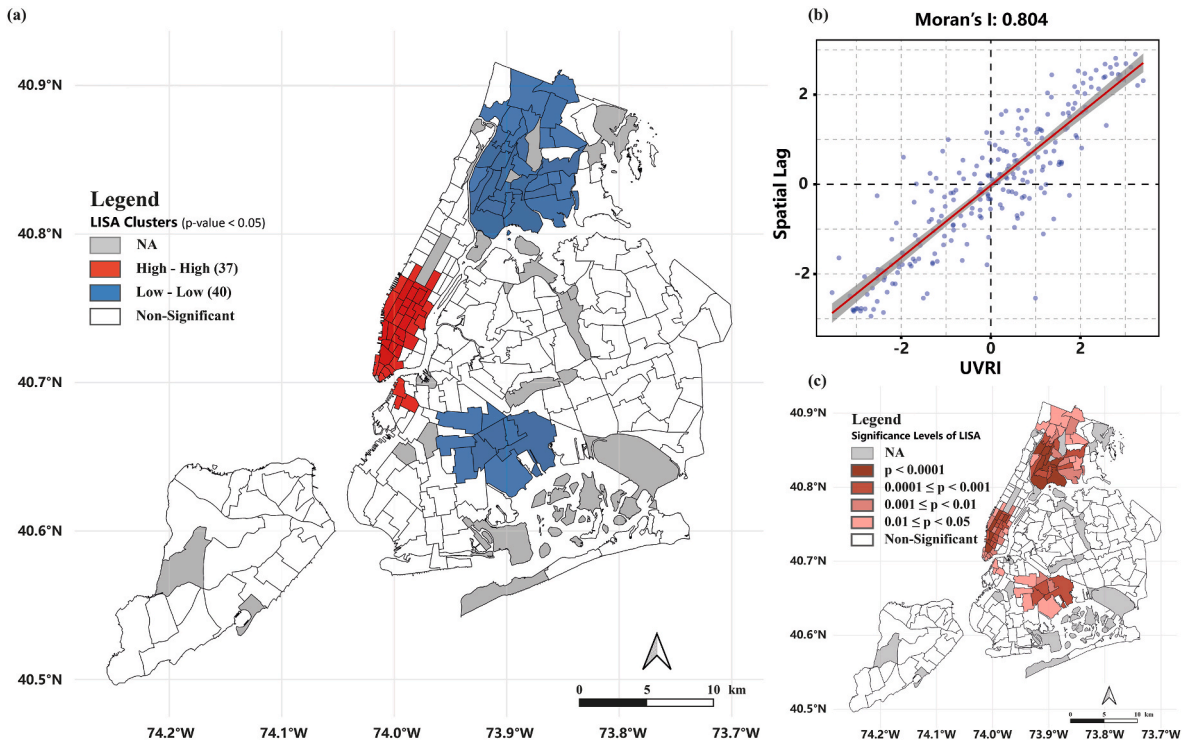

Fig. 8. Spatial autocorrelation of UVRI across NYC's TLC taxi zones: (a) LISA clusters ($p < 0.05$); (b) Moran's I scatter plot ($I = 0.804$); (c) LISA significance levels.

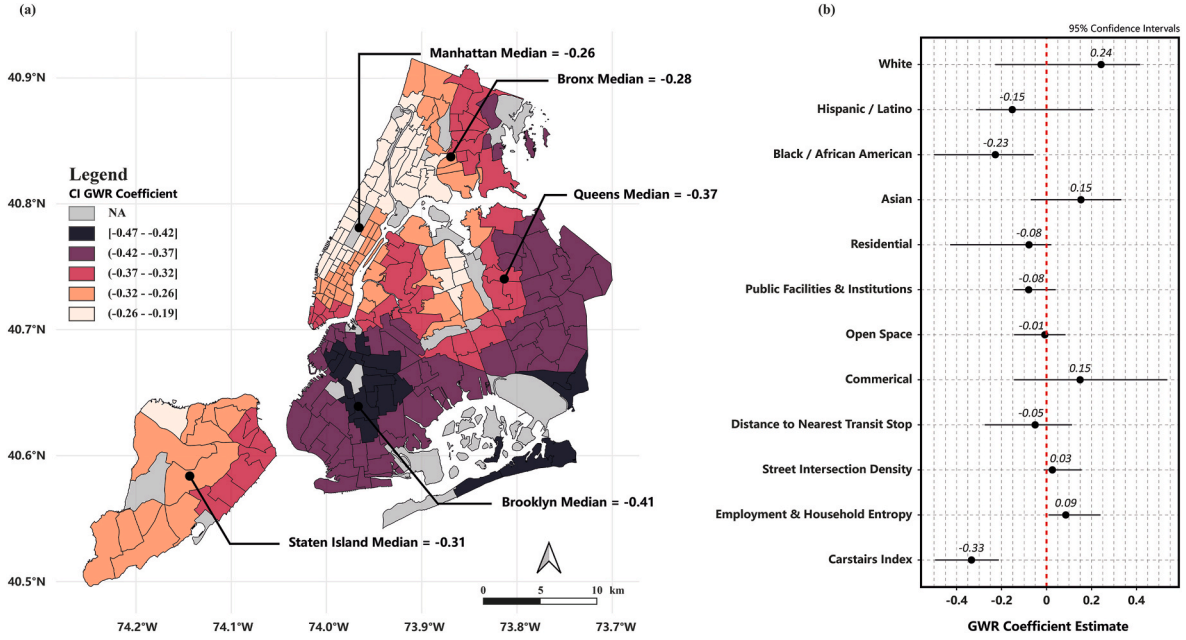

Fig. 9. Results of the adjusted GWR model for UVRI: (a) Spatial distribution of local GWR coefficients for the CI across NYC's TLC taxi zones with borough-stratified median values; (b) Coefficient distribution plot with 95 % confidence intervals, showing the influence of CI and covariates on UVRI.

Fig. 9(b) presents the distribution of GWR coefficient estimates with 95 % confidence intervals, illustrating the varying influences of socio-economic deprivation, demographic composition, built environment, and accessibility factors on UVRI across NYC taxi zones. The CI maintains its position as the top negative predictor with a median coefficient value of −0.33 that varies between −0.47 and −0.19, thereby validating the significant impact of socioeconomic deprivation on UVR. As a key demographic indicator, ethnic composition shows that White populations have positive links to UVRI, while Black and Hispanic or Latino populations have negative impacts, which indicate underlying socio-spatial disparities in resilience. Built environment factors, such as residential and institutional land use, generally have negative effects, while commercial areas exhibit a modest positive influence, suggesting that economic activity may aid in urban vibrancy recovery. Accessibility-related predictors, including distance to transit, street intersection density, and land-use diversity, show mixed but generally weaker associations.

6. Discussions

6.1. Mechanisms of urban vibrancy resilience

This study utilised the CI, a well-established composite method, as the foundation of the socioeconomic deprivation layer within our proposed analytical framework to construct a multidimensional deprivation measure across 234 TLC taxi zones in NYC. The spatial distribution of CI closely mirrors the city's entrenched socioeconomic landscape, which supports the contextual validity of the index. The southern Bronx, northern Manhattan, and northern Brooklyn have significantly high CI values, aligning with historical trends of concentrated poverty, unemployment, and housing instability recorded in these boroughs (ICPH, 2017; Johnson et al., 2022; Jonnes, 2022). This finding echoes existing research identifying these areas as epicentres of long-standing structural disadvantage (ICPH, 2017; Sharma et al., 2023; Liu et al., 2020; 2021). In contrast, zones with lower CI values, such as those on Staten Island, eastern Queens, and lower Manhattan, reflect more affluent urban contexts, where socioeconomic conditions are more stable, car ownership is more common, and access to essential services is less limited (Y. Huang & Li, 2022).

The UVRI findings showed significant spatial variation in taxi zones and boroughs throughout NYC. The downtown core of northeastern Brooklyn together with central and southern Manhattan areas along with Staten Island and Queens showed greater resilience because they recovered faster (RP) even though they experienced more intensive and rapid pandemic effects (IR and IP). The high recovery rate is especially noticeable for Staten Island, where all areas recovered rapidly and outperformed their previous vibrancy levels when entering the "new normal" stage. These conform to the fact that neighbourhoods with greater resilience often include economic and cultural hubs, dense and compact development, robust infrastructure, mixed land use, iconic landmarks, and good access to amenities and services (Chen et al., 2024; Sharifi & Yamagata, 2018). In contrast, areas with lower resilience are observed in Bronx, northern Manhattan, and eastern Brooklyn, which have historically been impacted by socioeconomic deprivation and uneven access to urban amenities (Liu et al., 2021). These neighbourhoods experienced slower and less significant effects, as well as delayed recoveries, despite some eventually attaining higher levels of urban vibrancy upon returning to normalcy. This result is consistent with claims by (Dorvil et al., 2023), who stated notable disturbances the communities encountered in regions like the South Bronx and sections of Brooklyn during the COVID-19 epidemic.

More importantly, our study identifies negative associations between CI and UVRI, indicating that regions with high deprivation levels tend to show diminished resilience. Typical factors of deprivation include overcrowded homes, severe poverty along with unemployed males, which align with widespread community vulnerabilities through insufficient resources and infrastructure, financial poverty and high living costs (Maroko et al., 2009; Wagmiller & Adelman, 2009; Hammarström, 1994). These socioeconomic conditions shape how well people and communities can manage and rebound from pandemic effects. The findings expand the current body of knowledge by demonstrating how people with low socioeconomic status face greater vulnerability during crises such as the COVID-19 pandemic (Patel et al., 2020). Less deprived areas with robust economies, agile businesses and extensive transit networks alongside concentrated healthcare systems demonstrate stronger resilience which shows the critical role of strategic urban planning and investment for crisis management and the development of resilient cities.

The GWR results further demonstrate spatial heterogeneity in the association between CI and UVRI. Every taxi zone showed negative CI coefficients while central Brooklyn and southeastern Queens demonstrated stronger negative patterns which correlated with higher deprivation and lower resilience. This demonstrates that resilience strategies should directly target the specific vulnerabilities linked to deprivation in these areas. The zones in Manhattan, the Bronx, and Staten Island revealed weaker associations, which suggests that institutional support and additional factors might help to mitigate negative effects beyond socioeconomic conditions. The impact of ethnicity-related variables on UVRI demonstrates the importance of designing resilience strategies that cater to the unique ethnic characteristics of different communities. Altogether, these findings point to the necessity of geographically sensitive policymaking to address socio-spatial disparities and to support equitable resilience across urban neighbourhoods.

6.2. Theoretical contribution

This study addresses the observed gaps and significantly contributes to urban resilience theory by explicitly integrating socio-spatial inequality with UVR. The utilisation of longitudinal FHV mobility data (2019–2023) to capture continuous urban vibrancy changes throughout the full spectrum of the pandemic, overcoming gaps in many studies that employed 'snapshot' approaches (Florida et al., 2021; Ntounis et al., 2022; Valenzuela-Levi et al., 2021). Additionally, by providing a thorough quantitative assessment of UVR at small-area resolution, our study reveals significant neighbourhood-level socio-spatial disparities, filling methodological gaps in resilience research typically addressed only qualitatively or at broader city-level scales (Xiao & Liu, 2023; Zhang & Wang, 2023). Lastly, the developed analytical framework is innovative and reproducible that has not been documented in prior research and can be easily adjusted to varying urban contexts and policy goals for exploring resilience disparities across different regions and countries.

6.3. Policy implications

The patterns in the empirical data strongly suggest that measures to enhance UVR should be targeted to deprived neighbourhoods, given the negative correlation of deprivation with UVRI. The GWR analysis also reveals that the deprivation effect is most strongly negative in Brooklyn and Queens, and relatively lesser negative in Manhattan, the Bronx, and Staten Island. This evidence supports a place-based resource allocation that focuses on the neighbourhoods where deprivation has the largest dampening effect on resilience, and then applies lessons from higher-resilience areas to uplift underperforming locations.

Areas in central and eastern Brooklyn and southeast Queens should, therefore, combine income and employment support, micro-grants and technical assistance for high streets and local businesses with bus priority and pedestrian and cycling links that make streets more accessible to activity generators. This recommendation aligns with both the significant negative correlations between UVRI and the unemployment and poverty domains of the CI and with the positive but weak effect of commercial use in the local modelling. If housing supply and affordability act as binding constraints in certain locations, then coordinate this package with the City of Yes for Housing Opportunity (Department of City Planning, 2024) to address overcrowding and stabilise tenure.

In the Bronx and northern Manhattan, where coldspots align with institutional assets, the focus should be on reliable public-realm management and the expansion of social infrastructure to maintain daily activity and reduce recovery lags. Citywide frameworks such as OneNYC 2050 (De Blasio et al., 2019) and the Community Parks Initiative (NYC Parks, 2020) offer suitable mechanisms for implementing these public-realm and community-asset investments. Higher-resilience areas, such as lower and central Manhattan, northwest Brooklyn, southern Staten Island, and northeast Queens, continue to serve as appropriate testbeds for piloting interventions such as flexible ground-floor activation before scaling out measures to low-resilience areas.

Any interventions should be consistent with the patterns in the UVR indicators. Higher resilience is related to a lower impact range and speed, and faster recovery. Measures in deprived neighbourhoods, therefore, should both minimise the extent of losses through, for example, targeted rent relief, utility arrears support, and business-

continuity grants, and accelerate the rebound through time-limited footfall-linked grants, streamlined pop-up permitting and street operations that directly support the local businesses. These recommendations follow from the component structure of the indicator, which makes clear how implementation can move the levers of resilience, rather than articulating broad ambitions.

Distributional and equity concerns must also be addressed. The local modelling suggests that ethnic composition also covaries with resilience in some neighbourhoods. White shares are positively associated, while Black and Hispanic or Latino shares are negatively associated. The implementation should adopt distributional targets by CI, monitor access to essential services and embed community co-design to ensure that benefits are delivered to groups over-represented in low-resilience zones.

6.4. Limitations and future works

This research contributes new insights into the concept of UVR. However, there are several limitations to this study. Firstly, we use urban mobility patterns as a main proxy to measure the concept of urban vibrancy. In reality, urban vibrancy can be a multi-dimensional and composite concept, with other factors such as social, economic, or cultural factors beyond physical movements, thus, solely relying on mobility data might miss these factors of urban vibrancy. More precisely, even though mobility data can inform about human movement behaviour, other types of behaviours like social engagement also constitute an important part of urban vibrancy (Tu et al., 2020). In addition, many attributes of urban vibrancy brought by those behaviours or perceived individually (e.g. sense of belonging to a community or living quality), might remain qualitative and not observable from mobility data, necessitating traditional survey or questionnaire approaches (Maroko et al., 2009). Because mobility data focuses on movement, it can lead to an overrepresentation of transportation hubs, potentially understating vibrancy in locations with less physical movement but strong social activity. Nevertheless, large-scale mobility data offers a quantitative perspective with advantages in coverage and spatiotemporal resolution. As a result, an increasing number of studies use urban mobility as a proxy that is more feasible to obtain while still representing an important part of urban vibrancy, especially when it comes to understanding cities' adaptation to such large-scale disruptions. Therefore, future research should include complementary quantitative and qualitative approaches for a more complete urban vibrancy measure.

Secondly, with respect to FHV trip data, only using this modality cannot represent the full modal split of urban mobility in the study area as we miss important travel patterns that do not occur through this modality (such as walking, cycling, or public transit trips). This is a crucial limitation, particularly given that FHV trips accounted for only a small fraction of all daily trips in NYC in 2019 (NYC Department of Transportation, 2019). We were constrained in our choice of modality as at the time of our research, there was limited open-source mobility data available that, like FHV data, has both a fine spatiotemporal resolution and a longitudinally consistent signal that extends for the entire period of the pandemic. Furthermore, FHV data may suffer from an intrinsic bias that under-represents populations with older ages, low income, or residing in the most deprived neighbourhoods (NYC DOT, 2022). This could be a critical bias that translates into an over-estimation of "stability" in more affluent areas and an oversight of more nuanced adaptive behaviours of communities in underprivileged neighbourhoods. One of our overarching aims is to develop an open-data analytical framework that is reproducible and transferable. Therefore, FHV data are only used as a proof-of-concept and, to our knowledge, the open-data framework could be built using the other available mobility datasets. Future research, therefore, should focus on the integration of different mobility data sources such as smartphone GPS logs, public transit records or even potentially qualitative mobility diaries to reduce this demographic bias and produce more holistic mobility insights across all socioeconomic levels.

Finally, in regard to the methodological choices made, some issues have to be taken into consideration that limit the generality of the analysis. First, the taxi zones in the vicinities of large airports and open spaces were removed from the analysis due to the lack of residents. This is coherent with the aim to measure and assess UVR in relation to socioeconomic deprivation. However, these spaces are also highly relevant urban structures that shape urban vibrancy, and future work can be devoted to understand the role of non-residential centrality (as mobility/economic attractors) for the resilience of residential zones in their vicinity. Second, although the CI is a sound measure and the GWR covariates included in the analysis account for important urban-related factors, future work can be improved by including more (and more detailed) urban contextual variables for a more comprehensive understanding of the resilience assessment (Chen & Liu, 2025). Finally, GWR is a method suitable for linear associations only, while real urban relationships are complex and probably non-linear, and future research can apply instead explainable AI or machine learning models (e.g., SHAP (SHapley Additive exPlanations)) to evaluate the feature importance of urban contexts for UVR.

7. Conclusion

This study systematically assessed socio-spatial disparities in UVR across NYC during pre-, peri-, and post-pandemic periods from 2019 to 2023 using longitudinal FHV data. A reproducible analytical framework was developed via indexation, spatial autocorrelation, and GWR modelling. Our findings consistently indicate a negative association between socioeconomic deprivation and resilience of urban vibrancy, both globally and locally, underscoring the need for targeted resilience strategies to address neighbourhood disparities. More importantly, this developed analytical framework can be readily applied in different urban contexts, which offers a flexible and effective toolkit for policymakers and urban planners to identify UVR disparities and design equitable interventions.

CRediT authorship contribution statement

Yunzhe Liu: Writing – review & editing, Writing – original draft, Visualization, Validation, Software, Resources, Methodology, Investigation, Formal analysis, Data curation, Conceptualization. **Meixu Chen:** Writing – review & editing, Writing – original draft, Validation, Supervision, Software, Project administration, Methodology, Investigation, Formal analysis, Conceptualization.

Declaration of generative AI and AI-assisted technologies in the writing process

During the preparation of this work the author(s) used ChatGPT 4.0 in order to improve the readability and language of the manuscript. After using this tool/service, the author(s) reviewed and edited the content as needed and take(s) full responsibility for the content of the publication.

Declaration of competing interest

The authors declare that they have no known competing financial interests or personal relationships that could have appeared to influence the work reported in this paper.

References

Acuti, D., Bellucci, M., & Manetti, G. (2020). Company disclosures concerning the resilience of cities from the Sustainable Development Goals (SDGs) perspective. *Cities*. https://doi.org/10.1016/j.cities.2020.102608

Afrin, S., Chowdhury, F. J., & Rahman, M. M. (2021). COVID-19 pandemic: Rethinking strategies for resilient urban design, perceptions, and planning. *Frontiers in Sustainable Cities, 3*.
Alizadeh, H., & Sharifi, A. (2021). Analysis of the state of social resilience among different socio-demographic groups during the COVID- 19 pandemic. *International Journal of Disaster Risk Reduction, 64*, Article 102514. https://doi.org/10.1016/j.ijdrr.2021.102514
Amirzadeh, M., Sobhaninia, S., & Sharifi, A. (2022). Urban resilience: A vague or an evolutionary concept? *Sustainable Cities and Society, 81*, Article 103853. https://doi.org/10.1016/j.scs.2022.103853
Anna, L., Blangiardo, M., Fortunato, L., Floud, S., De Hoogh, K., Fecht, D., Ghosh, R. E., Laszlo, H. E., Pearson, C., Beale, L., Beevers, S., Gulliver, J., Best, N., Richardson, S., & Elliott, P. (2013). Aircraft noise and cardiovascular disease near Heathrow airport in London: Small area study. *BMJ*. https://doi.org/10.1136/bmj.f5432
Anselin, L. (1995). Local indicators of spatial association—LISA. *Geographical Analysis, 27*, 93–115. https://doi.org/10.1111/j.1538-4632.1995.tb00338.x
Bautista-Puig, N., Benayas, J., Mañana-Rodríguez, J., Suárez, M., & Sanz-Casado, E. (2022). The role of urban resilience in research and its contribution to sustainability. *Cities*. https://doi.org/10.1016/j.cities.2022.103715
Blasio, B. de, & Jarmoszuk, A. H. (2020). *TLC factbook 2020*.
Buckingham, W. R., Bishop, L., Hooper-Lane, C., Anderson, B., Wolfson, J., Shelton, S., & Kind, A. J. H. (2021). A systematic review of geographic indices of disadvantage with implications for older adults. *JCI Insight*. https://doi.org/10.1172/jci.insight.141664
Carstairs, V., & Morris, R. (1990). Deprivation and health in scotland. *Health Bulletin*. https://doi.org/10.1136/pgmj.69.814.665-a
Chakraborty, L., Rus, H., Henstra, D., Thistlethwaite, J., Minano, A., & Scott, D. (2022). Exploring spatial heterogeneity and environmental injustices in exposure to flood hazards using geographically weighted regression. *Environmental Research*. https://doi.org/10.1016/j.envres.2022.112982
Chang, S., Pierson, E., Koh, P. W., Gerardin, J., Redbird, B., Grusky, D., & Leskovec, J. (2021). Mobility network models of COVID-19 explain inequities and inform reopening. *Nature*. https://doi.org/10.1038/s41586-020-2923-3
Chen, M., Arribas-Bel, D., & Singleton, A. (2019). Understanding the dynamics of urban areas of interest through volunteered geographic information. *Journal of Geographical Systems*. https://doi.org/10.1007/s10109-018-0284-3
Chen, M., & Liu, Y. (2025). Urban vibrancy resilience of New York City neighbourhoods across pre-, peri-, and post-pandemic periods via geodemographic classification. *Research Square*. https://doi.org/10.21203/rs.3.rs-6348202/v1
Chen, M., Liu, Y., Arribas-Bel, D., & Singleton, A. (2022). Assessing the value of user-generated images of urban surroundings for house price estimation. *Landscape and Urban Planning, 226*, Article 104486. https://doi.org/10.1016/J.LANDURBPLAN.2022.104486
Chen, M., Liu, Y., Ye, Z., Wang, S., & Zhang, W. (2024). Vivid London: Assessing the resilience of urban vibrancy during the COVID-19 pandemic using social media data. *Sustainable Cities and Society, 115*. https://doi.org/10.1016/j.scs.2024.105823
De Blasio, B., Fuleihan, D., Williams, D., & Zarrilli, D. A. (2019). OneNYC 2050: Building a strong and fair city. https://climate.cityofnewyork.us/wp-content/uploads/2024/09/OneNYC_2050_Strategic_Plan.pdf.
Department of City Planning. (2024). *City of Yes for housing opportunity*. New York City https://www.nyc.gov/site/planning/plans/city-of-yes/city-of-yes-housing-opportunity.page.
Dikeç, M. (2001). Justice and the spatial imagination. *Environment and Planning A, 33* (10). https://doi.org/10.1068/a3467
Dorvil, S., Nieves, C., Pierre, J., Valdez, J., Dannefer, R., Shiman, L. J., & Diallo, F. (2023). Disruption of healthcare in New York City during the COVID-19 pandemic: Findings from residents living in North and central Brooklyn, the South Bronx, and East and central harlem. *Journal of Primary Care and Community Health*. https://doi.org/10.1177/21501319231205992
Duan, J., Tian, G., Yang, L., & Zhou, T. (2021). Addressing the macroeconomic and hedonic determinants of housing prices in Beijing Metropolitan Area, China. *Habitat International*. https://doi.org/10.1016/j.habitatint.2021.102374
Fecht, D., Jones, A., Hill, T., Lindfield, T., Thomson, R., Hansell, A. L., & Shukla, R. (2018). Inequalities in rural communities: Adapting national deprivation indices for rural settings. *Journal of Public Health*. https://doi.org/10.1093/pubmed/fdx048
Florida, R., Rodríguez-Pose, A., & Storper, M. (2021). Cities in a post-COVID world. *Urban Studies, 60*(8). https://doi.org/10.1177/00420980211018072
Fotheringham, A. S., Brunsdon, C., & Charlton, M. (2002). *Geographically weighted regression: The analysis of spatially varying relationships*. Wiley.
Getis, A. (2007). Reflections on spatial autocorrelation. *Regional Science and Urban Economics*. https://doi.org/10.1016/j.regsciurbeco.2007.04.005
Green, M. A., García-Fiñana, M., Barr, B., Burnside, G., Cheyne, C. P., Hughes, D., Ashton, M., Sheard, S., & Buchan, I. E. (2021). Evaluating social and spatial inequalities of large scale rapid lateral flow SARS-CoV-2 antigen testing in COVID-19 management: An observational study of Liverpool, UK (November 2020 to January 2021). *The Lancet Regional Health - Europe*. https://doi.org/10.1016/j.lanepe.2021.100107
Gross, J. S., & Savitch, H. V. (2023). *New York*. Agenda Publishing.
Hammarström, A. (1994). Health consequences of youth unemployment-review from a gender perspective. *Social Science & Medicine*. https://doi.org/10.1016/0277-9536(94)90460-X
Haraguchi, M., Nishino, A., Kodaka, A., Allaire, M., Lall, U., Kuei-Hsien, L., Onda, K., Tsubouchi, K., & Kohtake, N. (2022). Human mobility data and analysis for urban resilience: A systematic review. *Environment and Planning B: Urban Analytics and City Science*. https://doi.org/10.1177/23998083221075634
Huang, Z., Chen, R., Xu, D., & Zhou, W. (2017). Spatial and hedonic analysis of housing prices in Shanghai. *Habitat International*. https://doi.org/10.1016/j.habitatint.2017.07.002
Huang, Y., & Li, R. (2022). The lockdown, mobility, and spatial health disparities in COVID-19 pandemic: A case study of New York City. *Cities*. https://doi.org/10.1016/j.cities.2021.103549
ICPH. (2017). *OnThe map: The dynamics of family homelessness in New York City*.
Jacobs, J. (1961). *The death and life of great American cities*. New York: Random House.
Jin, C., Xu, J., & Huang, Z. (2019). Spatiotemporal analysis of regional tourism development: A semiparametric geographically weighted regression model approach. *Habitat International*. https://doi.org/10.1016/j.habitatint.2019.03.011
Johnson, G. D., Checker, M., Larson, S., & Kodali, H. (2022). A small area index of gentrification, applied to New York City. *International Journal of Geographical Information Science*. https://doi.org/10.1080/13658816.2021.1931873
Jollife, I. T., & Cadima, J. (2016). Principal component analysis: A review and recent developments. In *Philosophical transactions of the royal society A: Mathematical, physical and engineering sciences*. https://doi.org/10.1098/rsta.2015.0202
Jolliffe, I. T. (2002). Principal component analysis. In *Springer series in statistics* (2nd ed.). Springer, 2nd ed.
Jonnes, J. (2022). *South Bronx rising: The rise, fall, and resurrection of an American city*. Fordham University Press (Third).
Khedmati Morasae, E., Derbyshire, D. W., Amini, P., & Ebrahimi, T. (2024). Social determinants of spatial inequalities in COVID-19 outcomes across england: A multiscale geographically weighted regression analysis. *SSM - Population Health*. https://doi.org/10.1016/j.ssmph.2024.101621
Kreyszig, E. (2011). *Advanced engineering mathematics (tenth)*. Wiley.
Liu, Y., Dajnak, D., Assareh, N., Beddows, A., Stewart, G., Holland, M., Evangelopoulos, D., Wood, D., Vu, T., Walton, H., Brand, C., Beevers, S., & Fecht, D. (2024). Impact of net zero policy scenarios on air pollution inequalities in England and Wales. *Environment International, 193*, Article 109065. https://doi.org/10.1016/j.envint.2024.109065
Liu, Y., Gu, T., Li, L., Cui, P., & Liu, Y. (2023). Measuring the urban resilience abased on geographically weighted regression (GWR) model in the post-pandemic era: A case study of jiangsu province, China. *Land*. https://doi.org/10.3390/land12071453
Liu, Y., Singleton, A., & Arribas-Bel, D. (2020). Considering context and dynamics: A classification of transit-orientated development for New York City. *Journal of Transport Geography*. https://doi.org/10.1016/j.jtrangeo.2020.102711
Liu, Y., Singleton, A., Arribas-bel, D., & Chen, M. (2021). Identifying and understanding road-constrained areas of interest (AOIs) through spatiotemporal taxi GPS data: A case study in New York City. *Computers, Environment and Urban Systems*. https://doi.org/10.1016/j.compenvurbsys.2020.101592
Liu, Y., Wang, X., Song, C., Chen, J., Shu, H., Wu, M., Guo, S., Huang, Q., & Pei, T. (2023). Quantifying human mobility resilience to the COVID-19 pandemic: A case study of Beijing, China. *Sustainable Cities and Society, 89*. https://doi.org/10.1016/j.scs.2022.104314
Maroko, A. R., Maantay, J. A., Sohler, N. L., Grady, K. L., & Arno, P. S. (2009). The complexities of measuring access to parks and physical activity sites in New York City: A quantitative and qualitative approach. *International Journal of Health Geographics*. https://doi.org/10.1186/1476-072X-8-34
Meerow, S., & Newell, J. P. (2019). Urban resilience for whom, what, when, where, and why? *Urban Geography*. https://doi.org/10.1080/02723638.2016.1206395
Meerow, S., Newell, J. P., & Stults, M. (2016). Defining urban resilience: A review. *Landscape and Urban Planning*. https://doi.org/10.1016/j.landurbplan.2015.11.011
Moran, P. A. P. (1950). Notes on continuous stochastic phenomena. *Biometrika*. https://doi.org/10.2307/2332142
Nan, C., & Sansavini, G. (2017). A quantitative method for assessing resilience of interdependent infrastructures. *Reliability Engineering & System Safety, 157*, 35–53. https://doi.org/10.1016/j.ress.2016.08.013
Newman, P., Beatley, T., & Boyer, H. (2017). Introduction: Urban resilience: Cities of fear and hope. In *Resilient cities*. https://doi.org/10.5822/978-1-61091-686-8_1
Nijman, J., & Wei, Y. D. (2020). Urban inequalities in the 21st century economy. *Applied Geography*. https://doi.org/10.1016/j.apgeog.2020.102188
Ntounis, N., Parker, C., Skinner, H., Steadman, C., & Warnaby, G. (2022). Tourism and hospitality industry resilience during the covid-19 pandemic: Evidence from england. *Current Issues in Tourism*. https://doi.org/10.1080/13683500.2021.1883556
Nunes, D. M., Tomé, A., & Pinheiro, M. D. (2019). Urban-centric resilience in search of theoretical stabilisation? A phased thematic and conceptual review. *Journal of Environmental Management*. https://doi.org/10.1016/j.jenvman.2018.09.078
NYC TLC. (2019). *TLC trip records user guide*.
NYC Department of Transportation. (2019). New York City mobility report. https://www.nyc.gov/html/dot/downloads/pdf/mobility-report-singlepage-2019.pdf.
NYC DOT. (2022). 2022 citywide mobility survey results. https://www.nyc.gov/html/dot/downloads/pdf/2022-cms-report.pdf.
NYC Parks. (2020). Community parks initiative. New York City https://www.nycgovparks.org/about/framework-for-an-equitable-future/community-parks-initiative.
NYC TLC. (2020). *COVID-19 impact on the NYC for-hire industry*.
Patel, J. A., Nielsen, F. B. H., Badiani, A. A., Assi, S., Unadkat, V. A., Patel, B., Ravindrane, R., & Wardle, H. (2020). Poverty, inequality and COVID-19: The forgotten vulnerable. *Public Health*. https://doi.org/10.1016/j.puhe.2020.05.006
Pereira, I. (2020). *NYC taxi drivers deliver food to those in need during coronavirus pandemic in new program*. Abc News. https://abcnews.go.com/US/nyc-taxi-drivers-deliver-food-coronavirus-pandemic-program/story?id=70241165.
Pfefferbaum, B., Pfefferbaum, R. L., & Van Horn, R. L. (2015). Community resilience interventions: Participatory, assessment-based, action-oriented processes. *American Behavioral Scientist*. https://doi.org/10.1177/0002764214550298

Ribeiro, P. J. G., & Pena Jardim Gonçalves, L. A. (2019). Urban resilience: A conceptual framework. *Sustainable Cities and Society*. https://doi.org/10.1016/j.scs.2019.101625

Roberton, J., Schmidt, S., & Stiles, R. (2020). *Emissions from the taxi and for-hire vehicle transportation sector in New York City*. TechRxiv.

Robinson, C., Lindley, S., & Bouzarovski, S. (2019). The spatially varying components of vulnerability to energy poverty. *Annals of the Association of American Geographers*. https://doi.org/10.1080/24694452.2018.1562872

Rojo, J., Rivero, R., Romero-Morte, J., Fernández-González, F., & Pérez-Badia, R. (2017). Modeling pollen time series using seasonal-trend decomposition procedure based on LOESS smoothing. *International Journal of Biometeorology*. https://doi.org/10.1007/s00484-016-1215-y

Schweitzer, F., Andres, G., Casiraghi, G., Gote, C., Roller, R., Scholtes, I., Vaccario, G., & Zingg, C. (2022). Modeling social resilience: QUESTIONS, answers, open problems. *Advances in Complex Systems, 25*(8). https://doi.org/10.1142/S021952592250014X

Sharifi, A., & Yamagata, Y. (2018). Resilient urban form: A conceptual framework. *Lecture Notes in Engineering*. https://doi.org/10.1007/978-3-319-75798-8_9

Sharma, R., Humphrey, J. L., Frueh, L., Kinnee, E. J., Sheffield, P. E., & Clougherty, J. E. (2023). Neighborhood violence and socioeconomic deprivation influence associations between acute air pollution and temperature on childhood asthma in New York City. *Environmental Research*. https://doi.org/10.1016/j.envres.2023.116235

Spielman, S. E., & Singleton, A. (2015). Studying neighborhoods using uncertain data from the American community survey: A contextual approach. *Annals of the Association of American Geographers*. https://doi.org/10.1080/00045608.2015.1052335

Su, S., Gong, Y., Tan, B., Pi, J., Weng, M., & Cai, Z. (2017). Area social deprivation and public health: Analyzing the spatial non-stationary associations using geographically weighed regression. *Social Indicators Research*. https://doi.org/10.1007/s11205-016-1390-6

Su, S., Xiao, R., & Zhang, Y. (2012). Multi-scale analysis of spatially varying relationships between agricultural landscape patterns and urbanization using geographically weighted regression. *Applied Geography*. https://doi.org/10.1016/j.apgeog.2011.06.005

Thompson, C. N., Baumgartner, J., Pichardo, C., Toro, B., Li, L., Arciuolo, R., Chan, P. Y., Chen, J., Culp, G., Davidson, A., Devinney, K., Dorsinville, A., Eddy, M., English, M., Fireteanu, A. M., Graf, L., Geevarughese, A., Greene, S. K., Guerra, K., … Fine, A. (2020). COVID-19 outbreak — New York City, february 29–june 1, 2020. *MMWR. Morbidity and Mortality Weekly Report*. https://doi.org/10.15585/mmwr.mm6946a2

Tu, W., Zhu, T., Xia, J., Zhou, Y., Lai, Y., Jiang, J., & Li, Q. (2020). Portraying the spatial dynamics of urban vibrancy using multisource urban big data. *Computers, Environment and Urban Systems*. https://doi.org/10.1016/j.compenvurbsys.2019.101428

Valenzuela-Levi, N., Echiburu, T., Correa, J., Hurtubia, R., & Muñoz, J. C. (2021). Housing and accessibility after the COVID-19 pandemic: Rebuilding for resilience, equity and sustainable mobility. *Transport Policy*. https://doi.org/10.1016/j.tranpol.2021.05.006

Wagmiller, J. R. L., & Adelman, R. M. (2009). Childhood and intergenerational poverty: The long-term consequences of growing up poor. In *National center for children in poverty*.

Wang, Y., Dong, L., Liu, Y., Huang, Z., & Liu, Y. (2019). Migration patterns in China extracted from mobile positioning data. *Habitat International*. https://doi.org/10.1016/j.habitatint.2019.03.002

Wang, H., Xu, Y., & Wei, X. (2023). Rural resilience evaluation and influencing factor analysis based on geographical detector method and multiscale geographically weighted regression. *Land*. https://doi.org/10.3390/land12071270

Wang, M., & Wang, X. S. (2006). Finding the plateau in an aggregated time series. In *Proceedingsof the 7th international conference on Advances in Web-Age Information Management (WAIM '06)* (pp. 325–336). Berlin, Heidelberg: Springer-Verlag. https://doi.org/10.1007/11775300_28.

Xiao, L., & Liu, J. (2023). Exploring non-linear built environment effects on urban vibrancy under COVID-19: The case of Hong Kong. *Applied Geography*. https://doi.org/10.1016/j.apgeog.2023.102960

Yan, X., Pei, T., Gong, X., Fu, Z., & Liu, Y. (2025). Assessing differences in work intensity resilience to pandemic outbreaks using large-scale mobile phone data. *International Journal of Applied Earth Observation and Geoinformation, 136*(December 2024), Article 104343. https://doi.org/10.1016/j.jag.2024.104343

Yue, Y., Zhuang, Y., Yeh, A. G. O., Xie, J. Y., Ma, C. L., & Li, Q. Q. (2017). Measurements of POI-based mixed use and their relationships with neighbourhood vibrancy. *International Journal of Geographical Information Science*. https://doi.org/10.1080/13658816.2016.1220561

Zhang, J., & Wang, T. (2023). Urban resilience under the COVID-19 pandemic: A quantitative assessment framework based on system dynamics. *Cities, 136*(104265), Article 104265. https://doi.org/10.1016/j.cities.2023.104265